Regular paper

Water Sorption Isotherm and Critical Water Activity of Amorphous Water-Soluble Carbohydrates Characterized by the Glass Transition Temperature

Yuichi Kashiwakura,[1,2] Tomochika Sogabe,[1,2] Sukritta Anantawittayanon,[1]
Takumi Mochizuki,[1] and Kiyoshi Kawai[1,†]

[1] *Program of Food and AgriLife Science, Graduate School of Integrated Sciences for Life, Hiroshima University*
(1−4−4 Kagamiyama, Higashi-Hiroshima, Hiroshima 739−8528, Japan)
[2] *Research and Development Center, B Food Science Co., Ltd.*
(24−12 Kitahama-machi, Chita, Aichi 478−0046, Japan)

Abstract: Water-soluble carbohydrates commonly exist in an amorphous state in foods and undergo glass-rubber transition (glass transition) at the glass transition temperature (T_g). The critical water content (W_c) and critical water activity (a_{wc}) are the water content and water activity (a_w) at which the glass transition occurs at 298 K (typical ambient temperature), respectively. For amorphous water-soluble carbohydrates, W_c can be predicted from the T_g of anhydrous solid (T_{gs}) using previously reported equations. However, an approach for predicting a_{wc} is still lacking. This study aimed to establish an a_{wc}-predictive approach for amorphous water-soluble carbohydrates based on T_{gs}. First, the water sorption isotherms of four hydrogenated starch hydrolysates were investigated, and the results were analyzed using the Guggenheim–Anderson–de Boer (GAB) model. Second, the effect of T_{gs} on the GAB parameters (C, K, and W_m) was evaluated using the T_{gs} values reported in previous literatures. C and W_m decreased and increased logarithmically, respectively, with increasing $1/T_{gs}$. K was fixed to 1 (constant), as it showed little variation. These results enabled the prediction of the GAB parameters from T_{gs}. The GAB model could then predict a_{wc} from W_c, which was determined using the previously established equations. The predicted a_{wc} values were in good agreement with the experimentally determined a_{wc}. Additionally, we demonstrated that this a_{wc}-prediction approach is also applicable to amorphous water-soluble electrolytes and partially water-insoluble carbohydrates. Thus, this approach can be used for the quality control of amorphous water-soluble carbohydrates and carbohydrate-based foods.

Key words: glass transition, water sorption, water activity, hydrogenated starch hydrolysate, amorphous carbohydrate

INTRODUCTION

Water-soluble carbohydrates are commonly present in an amorphous form in food products and undergo glass-rubber transition (glass transition) at their glass transition temperature (T_g). At temperatures below T_g, amorphous carbohydrates in food matrices exist in the glassy state and have a hard, brittle, and/or crisp texture [1,2]. Meanwhile, above T_g, amorphous carbohydrates become rubbery and have a texture that is soft, ductile, and/or sticky. Caking (aggregation) of amorphous carbohydrate-based powders readily occurs in the rubbery state [3–8]. Because the T_g of amorphous hydrophilic carbohydrates decreases with increasing water content and/or water activity (a_w) owing to water plasticization, water sorption can result in glass transition even at a constant temperature. The water content and a_w at which glass transition can occur at ambient temperature (commonly 298 K) are termed as the critical water content (W_c) and critical water activity (a_{wc}), respectively [9–12], which are useful parameters for the quality control of amorphous water-soluble carbohydrates and carbohydrate-based foods.

The effect of water content on the T_g of amorphous materials is described by the Gordon-Taylor (GT) equation (Eq. 1),

$$T_g = \frac{M_s T_{gs} + k(1-M_s) T_{gw}}{M_s + k(1-M_s)} \quad \text{(Eq. 1)}$$

where M_s is the mass fraction of the solid, T_{gs} is the T_g of the anhydrous solid (K), T_{gw} is the T_g of water (K), and k is a constant (dimensionless). T_{gw} can be set to 136 K [13,14]. With two constants (T_{gsw} and k), T_g-curve (water content-dependence of T_g) and W_c can be determined using the GT equation. In addition, a_{wc} can be determined using the Guggenheim–Anderson–de Boer (GAB) water sorption equation (Eq. 2),

$$W = \frac{W_m C K a_w}{(1-K a_w)(1+(C-1) K a_w)} \quad \text{(Eq. 2)}$$

where W and W_m are the equilibrium water content (g/g-DM,

†Corresponding author (Tel. & Fax. +81−82−424−4344, E-mail: kawai@hiroshima-u.ac.jp, ORCID ID: https://orcid.org/0000-0001-9828-9030)

dry matter) and monolayer water content (g/g-DM), respectively; C is a factor correcting the sorption properties of the monolayer with respect to the bulk liquid; and K is a factor correcting the sorption properties of the multilayer with respect to the bulk liquid. From the GAB equation with three parameters (W_m, C, and K), W_c can be converted to a_{wc}.

For amorphous water-soluble carbohydrates, k in the GT equation (Eq. 1) can be predicted from T_{gs} (K) using the following empirical equation [12]:

$$k = 0.0293\, T_{gs} - 4.39 \qquad \text{(Eq. 3)}$$

After determining the T_{gs} and k, W_c can be predicted by rearranging the GT equation (Eq. 1) as follows:

$$M_{sc} = \frac{162\, k}{162\, k + T_{gs} - 298} \qquad \text{(Eq. 4)}$$

$$W_c = \frac{1 - M_{sc}}{M_{sc}} \qquad \text{(Eq. 5)}$$

where M_{sc} is the mass fraction of the solute at $T_g = 298$ K. The T_{gs} values of various amorphous water-soluble carbohydrates have been widely reported by previous studies. If no data are available in the literature, the T_{gs} of such carbohydrates can be easily evaluated using differential scanning calorimetry (DSC). Additionally, the T_{gs} of an amorphous water-soluble carbohydrate mixture can be predicted from the T_{gs} and ΔC_p (heat capacity change induced by glass transition) of the individual components [11]. Thus, the fact that W_c can be predicted from T_{gs} has an important basis in food quality control. However, no study has reported an approach for predicting a_{wc}. Because the quality of food and food ingredients is commonly controlled by a_w, determining a_{wc} is more important than determining W_c. Like W_c, it is useful if a_{wc} can be also predicted by T_{gs}. The water sorption behavior is affected by T_{gs} [15,16], as shown in Fig. 1; further explanation is provided in Appendix a. Thus, there is a possibility that GAB parameters can be characterized by T_{gs}.

The present study aimed to establish a method to predict the a_{wc} of amorphous water-soluble carbohydrates from their T_{gs}. First, we evaluated the water sorption isotherms of four types of hydrogenated starch hydrolysate (HSH) and analyzed the results using the GAB model. Second, the effect of T_{gs} on the GAB parameters of amorphous water-soluble carbohydrates was investigated using T_{gs} values reported in the literature, and an a_{wc}-predictive approach was proposed. Finally, we assessed the applicability of this a_{wc}-prediction method to amorphous water-soluble electrolytes and partially water-insoluble carbohydrates.

MATERIALS AND METHODS

Materials. Four types of HSH syrup (water content 30 %) were obtained from B Food Science Co., Ltd. (Aichi, Japan). The sugar alcohol composition of these HSHs [11] is shown in Supplemental Data (Table S1; see J. Appl. Glycosci. Web site). Based on which, they were categorized as low molecular weight (Mw)- (LoHSH), lower-middle Mw- (LMiHSH), middle Mw- (MiHSH), and high Mw-enriched HSH (HiHSH).

Preparation of freeze-dried amorphous powder samples. Amorphous LoHSH, LMiHSH, MiHSH, and HiHSH powder samples were prepared by freeze-drying their aqueous solutions. Briefly, the HSHs were diluted to 20 % (w/w) by adding distilled water and frozen in a freezer at 253 K. The frozen samples were then transferred to a pre-cooled chamber and freeze-dried at approximately 11 Pa by increasing the temperature from 238 to 278 K gradually over 48 h. Subsequently, the freeze-dried solids were ground manually to obtain the powders. The LoHSH solid was ground in liquid nitrogen in an aluminum container to obtain fine powder. The freeze-dried samples were then stored in a refrigerator until use.

Water sorption isotherms. Freeze-dried amorphous powder samples (0.5 g) were placed in an aluminum dish (diameter 40 mm), and the residual moisture in the samples was removed by vacuum-drying at 80 ºC (stage temperature) for 6 h. Next, the dry samples were maintained at 298 K for longer than 7 days in a desiccator with saturated salts: Mg(NO₃)₂ ($a_w = 0.529$), NaBr ($a_w = 0.576$), KI ($a_w = 0.688$), NaCl ($a_w = 0.753$), and KCl ($a_w = 0.843$). We have previously reported the T_g and equilibrium water content of the HSHs in the low a_w-region (0−0.432) [11]. The water content in the
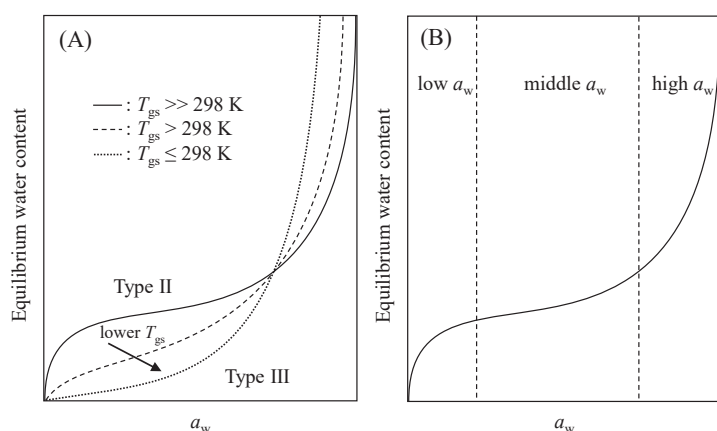
Fig. 1. Water sorption isotherm of amorphous water-soluble carbohydrates with varying T_{gs} (A), and three regions in the type II isotherm (B).
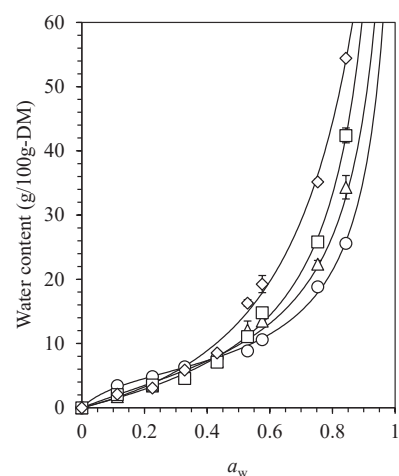
Fig. 2. Water sorption isotherm of LoHSH, LMiHSH, MiHSH, and HiHSH.
The solid curves were obtained by fitting the GAB model (Eq. 2) to the data. The values are expressed as the mean ± SD ($n = 3$).

Table 1. Glass transition and water sorption properties of amorphous water-soluble carbohydrates.

Sample	C	K	W_m (g/100g)	T_{gs} (K)	k	W_c (g/100g)	a_{wc}	Ref.
LoHSH	0.572	0.853	25.583	283.5	2.23[a]	NA	NA	11
LMiHSH	1.424	0.965	9.156	324.9	4.31[a]	2.43[b]	0.173[c]	11
MiHSH	2.725	0.946	7.257	344.8	12.13[a]	3.95[b]	0.227[c]	11
HiHSH	9.639	0.949	5.325	402.0	24.25[a]	8.74[b]	0.482[c]	11
Maltodextrin (MD)	9.192	0.995	4.3	435.8	9.00	9.4	0.575	4
Mango solute (MS)[d]	1.686	0.920	16.1	310.4	3.86	1.9	0.074	3
MS-MD (0.2 : 0.8)	2.303	0.922	6.4	366.1	7.18	5.8	0.345	3
MS-MD (0.4 : 0.6)	2.268	0.958	8.1	335.3	5.57	4.1	0.215	3
MS-MD (0.6 : 0.4)	2.640	0.950	9.8	325.5	4.95	3.4	0.160	3
MS-MD (0.8 : 0.2)	3.414	0.915	13.0	320.3	4.07	3.3	0.120	3
Maltose	4.05	1.085	5.33	368.6	7.4	5.89[b]	0.337[c]	17
Glucose-MD (0.2 : 0.8)	6.40	0.933	6.47	370.1	8.11	7.20	0.343	7
Inulin (low MW)	3.66	0.944	6.87	384.4	6.43	8.29[b]	0.431[c]	18
Inulin (native)	6.95	0.852	6.77	398.0	5.93	10.41[b]	0.525[c]	18

[a] The value was calculated by the approximated Couchman-Karasz model [11]. [b] The value was calculated by the Gordon–Taylor model with T_{gs} and k (Eq. 1). [c] The value was calculated by the Guggenheim, Anderson, and de Boer model with W_c (Eq. 2). [d] Water-soluble materials (manly sucrose, glucose, and fructose) were extracted from mango puree [4].

samples was determined gravimetrically by oven-drying at 378 K for 16 h. The measurements were performed in triplicate, and the results were averaged.

Statistical analysis. Regression analyses were conducted using the root mean squared error (RMSE), mean absolute percentage error (MAPE), and coefficient of determination (R^2).

RESULTS AND DISCUSSION

Water sorption isotherms of amorphous HSHs.

Water sorption isotherms of the HSH samples maintained at 298 K are shown in Fig. 2. LMiHSH, MiHSH, and HiHSH exhibited "type II" water sorption isotherms (Appendix a). Their T_{gs} values were considerably higher than 298 K (Table 1); thus, glass transition occurred at a certain a_w in the water sorption isotherms. However, LoHSH exhibited a "type III" water sorption isotherm (Appendix a). The T_{gs} of LoHSH (283.5 K) was lower than 298 K (Table 1); thus, a rubbery or liquid state was observed in all the a_w-region. Type III is commonly observed for amorphous water-soluble carbohydrates that have a T_{gs} lower than or close to 298 K; thus, a_{wc} cannot be defined intrinsically for these materials (Appendix a). LoHSH exhibited a type III curve like we expected. Thus, a_{wc}-prediction based on T_{gs} was conducted for only the samples showing type II isotherms (LMiHSH, MiHSH, and HiHSH).

Effect of T_{gs} on the GAB parameters of amorphous water-soluble carbohydrates.

To establish an a_{wc}-predictive approach based on T_{gs}, the GAB and GT parameters for amorphous water-soluble carbohydrates were taken from the literature [3,4,7,11,17,18] and are listed in Table 1. GAB parameters are very sensitive to experimental values; a small deviation in the experimental values can cause a large difference in the GAB parameters [4,19,20]. In addition, the water contents at each a_w are different between water sorption and water desorption (i.e., hysteresis effect). Therefore, the water content in samples needs to be removed fully prior to water sorption. However, these problems are not always elucidated in the literature. To avoid employing uncertain data, we only included the data

reported by our research group at this stage and the data reported by other studies were applied later for comparison.

The relationship between C and T_{gs} is shown in Fig. 3A. The C values increased with increasing T_{gs}. The effect of the temperature on C can be analyzed using the Arrhenius-type (or van't Hoff-type) equation [21–24]:

$$C = C_0 \exp\left(\frac{\Delta H_C}{RT}\right) \quad \text{(Eq. 6)}$$

where T and R are absolute temperature and gas constant, respectively, and C_0 and ΔH_C are pre-exponential factor and activation energy, respectively. Temperature is directly proportional to molecular mobility; the higher the temperature, the higher the molecular mobility. Conversely, T_{gs} is inversely proportional to molecular mobility; the higher the T_{gs}, the lower the molecular mobility at a constant temperature (298 K in this study). In other words, T and T_{gs} are interchangeable parameters that reflect molecular mobility. Accordingly, the Arrhenius-type plot for C (Eq. 6) can be rearranged as follows:

$$C = C_0^* \exp\left(\frac{C^*}{T_{gs}}\right) \quad \text{(Eq. 7)}$$

where C_0^* and C^* are constants. This equation is referred to as "T_g-based Arrhenius-like equation" in this paper.

The T_g-based Arrhenius-like plot ($\ln C$ vs. $1/T_{gs}$) for amorphous water-soluble carbohydrates is shown in Fig. 3B. There was a clear linearity in the plot ($R^2 = 0.857$), and C^* (slope) and $\ln C_0^*$ (intercept) values were determined to be -2022.7 and 6.9514, respectively, from the linearity (Eq. 7). Linearity also describes the solid curve shown in Fig. 3A.

The effect of temperature on K has also been analyzed using the Arrhenius-type equation previously [21–24]:

$$K = K_0 \exp\left(\frac{\Delta H_K}{RT}\right) \quad \text{(Eq. 8)}$$

where K_0 and ΔH_K are the pre-exponential factor and activation energy, respectively. Thus, it is expected that the T_g-based Arrhenius-like equation can be also applied to K in addition to C (Eq. 7). However, there was little variation in K values of the amorphous water-soluble carbohydrates (Table 1), and mean ± SD of the K values was confirmed to
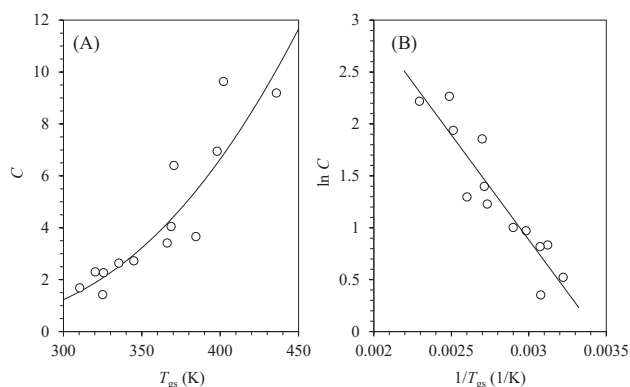
Fig. 3. Effect of T_{gs} on the C of amorphous water-soluble carbohydrates (A) and T_g-based Arrhenius-like plot of the C (B).

The values are listed in Table 1. The relationship between $\ln C$ and $1/T_{gs}$ (Fig. 3B) was analyzed by the linear fitting, and C^* (slope) and $\ln C_0^*$ (intercept) values were determined. The linear proportion was transformed to C vs. T_{gs} as solid line in Fig. 3A.

Fig. 4. Effect of T_{gs} on the W_m of amorphous water-soluble carbohydrates (A) and T_g-based Arrhenius-like plot of the W_m (B).

The values are listed in Table 1. The relationship between $\ln W_m$ and $1/T_{gs}$ (Fig. 4B) was analyzed by the linear fitting, and W_m^* (slope) and $\ln W_{m0}^*$ (intercept) values were determined. The linear proportion was transformed to W_m vs. T_{gs} as solid line in Fig. 4A.

be 0.942 ± 0.057 ($n = 13$). To simplify the a_{wc}-predictive approach, K was fixed to 1 (constant) for amorphous water-soluble carbohydrates.

When K is fixed to 1, the GAB model is equivalent to the Brunauer–Emmett–Teller (BET) model. The BET model is commonly employed to analyze water sorption behavior up to the intermediate a_w-region [17]. Because the a_{wc} values of amorphous water-soluble carbohydrates are almost in the a_w-range applied by the BET model (Table 1), the setting of K as 1 simplified the a_{wc}-predictive approach. Electrolyte polymers (e.g., proteins) and samples containing water-insoluble materials and/or parts have been reported to exhibit a much lower value of K than 1 [7,25]. However, this study focused only on water-soluble carbohydrates, which simplified the approach.

The temperature dependence of W_m has often been undetermined by previous studies, although there are some examples in which the Arrhenius-type equation has been applied [19,21]. This will be because the monolayer water content is independent of temperature, and temperature has a negligible effect on the surface area of materials. In contrast, W_m intrinsically depends on T_{gs} (Appendix a), because higher the T_{gs}, larger is the molar mass [11,18] and thus lower the surface area per g-DM. In other words, it is expected that a higher T_{gs} corresponds to a lower W_m.

The effect of T_{gs} on the W_m of amorphous water-soluble carbohydrates is shown in Fig. 4A. As expected, W_m decreased with increasing T_{gs}. As discussed above, the effect of T_{gs} on W_m can be analyzed using the T_g-based Arrhenius-like equation.

$$W_m = W_{m0}^* \exp\left(\frac{W_m^*}{T_{gs}}\right) \qquad \text{(Eq. 9)}$$

where W_{m0}^* and W_m^* are constants. The T_g-based Arrhenius-like plot ($\ln W_m$ vs. $1/T_{gs}$) is shown in Fig. 4B. Good linearity was observed in the plot ($R^2 = 0.812$), and W_m^* (slope) and $\ln W_{m0}^*$ (intercept) values were determined to be 1159 and -5.830, respectively. Linearity also describes the solid curve shown in Fig. 4A.

Although the physical significance of the constants (C^*, C_0^*, W_m^*, and W_{m0}^*) in the T_g-based Arrhenius-like equation is unclear at present, the T_g-based Arrhenius-like plot can be
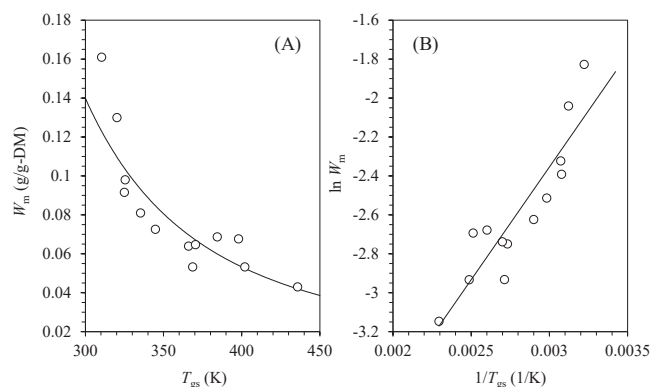
effectively used to express the effect of T_{gs} on the C and W_m of amorphous water-soluble carbohydrates. This is a valuable result for establishing an a_{wc}-predictive approach based on T_{gs}.

Applicability of the a_{wc}-predictive approach to amorphous water-soluble carbohydrates.

As C and W_m can be predicted using T_{gs}, a_{wc} can also be predicted using T_{gs}. Briefly, k was obtained using Eq. 3 from T_{gs}, and then, W_c was obtained using Eq. 5 using T_{gs} and k. Meanwhile, C and W_m were obtained using Eqs. 7 and 9, respectively, using T_{gs}. Thereafter, W_c was converted to a_{wc} using Eq. 2 with obtained C and W_m values. Subsequently, using the a_{wc}-predictive approach, a_{wc} was calculated from the experimentally determined T_{gs} listed in Table 1 [3,4,7,11,17,18]. The relationship between the experimentally determined a_{wc} and the predicted a_{wc} is shown in Fig. 5. The calculated a_{wc} values were in good agreement with the predicted a_{wc} values (RMSE = 0.035, MAPE = 9.05, and $R^2 = 0.948$; $n = 13$).

To further validate our proposed method, the applicability of the a_{wc}-prediction approach to other water-soluble carbohydrates reported in the literature was tested. The experimentally determined T_{gs} and a_{wc} and predicted a_{wc} are listed in Supplemental Data (Table S2; see J. Appl. Glycosci. Web site) [9,10,26–28]. The relationship between the experimentally determined and predicted a_{wc} is shown in Fig. 6. There was relatively good agreement between the values (RMSE = 0.058, MAPE = 16.7, $R^2 = 0.906$, $n = 12$). Based on these results, we concluded that the a_{wc}-predictive approach based on T_{gs} can successfully determine the a_{wc} of amorphous water-soluble carbohydrates.

The a_{wc}-predictive approach can predict the GAB parameters, which implies that water sorption isotherm can also be predicted from T_{gs}. For confirmation, we evaluated the relationship between the experimentally determined and predicted water content at each a_w (Fig. 7) and found the values were in moderate agreement (RMSE = 7.66, MAPE = 21.2, and $R^2 = 0.777$; $n = 90$). A large difference between the calculated and predicted values was observed in the high-water content (high a_w) region. This is because the BET model (applicable in the low and intermediate a_w-regions)
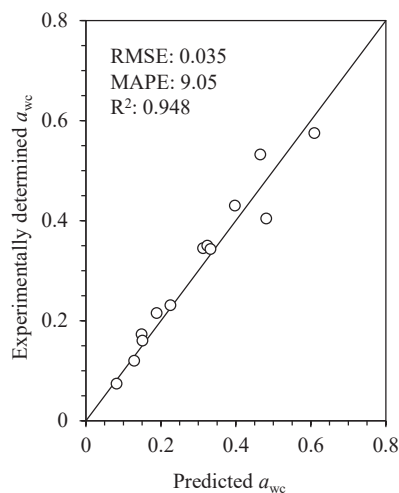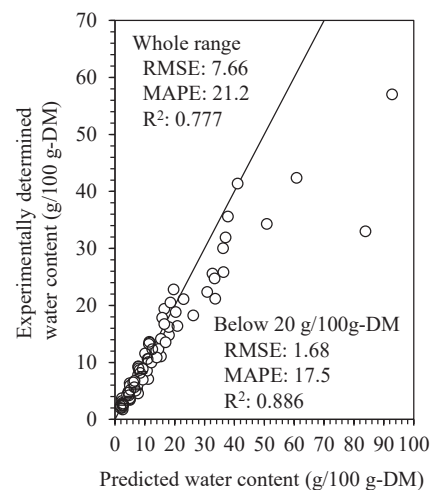
Fig. 5. Relationship between experimentally determined a_{wc} and predicted a_{wc} of amorphous water-soluble carbohydrates.

The experimentally determined a_{wc} values are listed in Table 1.
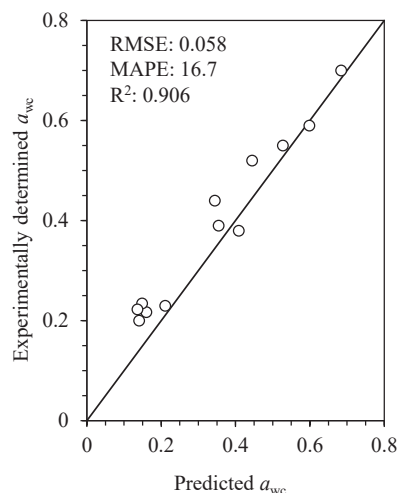
Fig. 6. Relationship between a_{wc} values obtained from previous literature and predicted a_{wc} values of amorphous water-soluble carbohydrates.

The values are listed in Supplemental Data (Table S2; see J. Appl. Glycosci. Web site).

Fig. 7. Relationship between experimentally determined water content and predicted water content of amorphous water-soluble carbohydrates at each a_w.

The GAB parameters reflecting experimentally determined water content are listed in Table 1.

was applied as the predictive approach. The prediction was greatly improved when the water content range was limited to < 20 g/100 g-DM (RMSE = 1.68, MAPE = 17.5, and R^2 = 0.886; n = 73).

Effect of amorphous water-soluble electrolytes and water-insoluble carbohydrates on the a_{wc}-predictive approach.

The a_{wc}-predictive approach was established with the assumption that the materials were amorphous water-soluble carbohydrates. Thus, we evaluated whether this a_{wc}-predictive approach is also applicable to other carbohydrates and carbohydrate-based materials.

The experimentally determined T_{gs} and a_{wc} and predicted a_{wc} of the amorphous electrolytes and carbohydrate-electrolyte mixtures are listed in Supplemental Data (Table S3; see J. Appl. Glycosci. Web site) [17,29]. The relationship
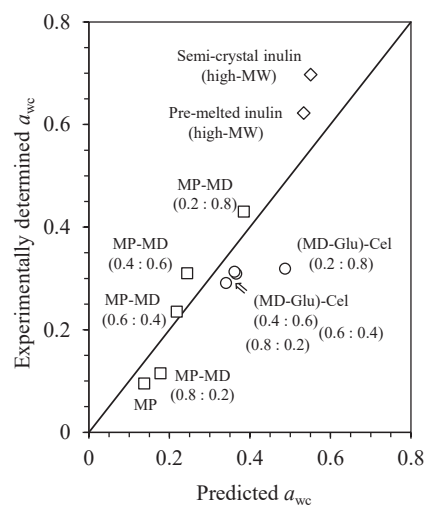
between the experimentally determined and predicted a_{wc} is shown in Fig. 8. The experimental and predicted a_{wc} values of calcium maltobionate (CaMb) and CaMb-maltose mixtures were almost similar. CaMb is composed of a divalent cation (Ca^{2+}) and two maltobionate ions. Maltobionate consists of glucose and gluconate. Because the CaMb and CaMb-maltose systems comprise carbohydrate and carbohydrate-related (hydrogen-bonding system) parts, the contribution of electrostatic interactions in them is weak. Thus, the a_{wc}-predictive approach established by amorphous water-soluble carbohydrates can be applied to them as well. The predicted a_{wc} of HMb (maltobionic acid), however, showed a large deviation from its experimentally determined value owing to large electrostatic interactions.

The experimentally determined T_{gs} and a_{wc} and the predicted a_{wc} for partially water-insoluble carbohydrates are listed in
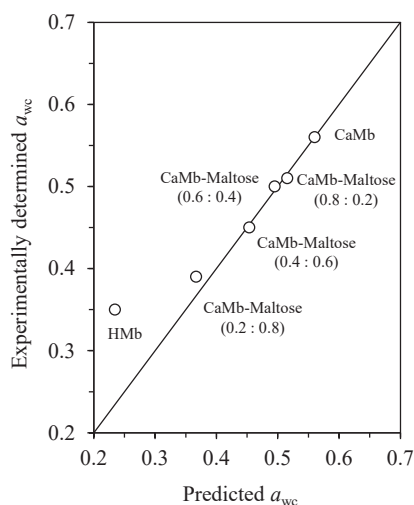
Fig. 8. Relationship between experimentally determined a_{wc} and predicted a_{wc} of amorphous electrolytes and carbohydrate-electrolyte mixtures.

The values are listed in Supplemental Data (Table S3; see J. Appl. Glycosci. Web site).

Fig. 9. Relationship between experimentally determined a_{wc} and predicted a_{wc} of partially water-insoluble carbohydrates.

The values are listed in Supplemental Data (Table S4; see J. Appl. Glycosci. Web site).

Supplemental Data (Table S4; see J. Appl. Glycosci. Web site)[4,7,18]. The relationship between the experimentally determined a_{wc} and the predicted a_{wc} is shown in Fig. 9. The higher the water-insoluble content, the larger the deviation in the prediction. For example, the values of semi-crystalline inulin (high-MW), which contains water-insoluble (crystal) parts, showed a larger deviation than those of pre-melted inulin (high-MW). In the case of (maltodextrin (MD)-glucose)-cellulose samples (MD-glucose mixture at 0.2 dry weight fraction of glucose was mixed with crystalline cellulose at 0.8, 0.6, 0.4, and 0.2 dry weight fractions of cellulose), the a_{wc} of the sample containing 0.8 dry weight fraction of cellulose showed the largest deviation from the predicted value. These large deviations originate from the different physical significance of water content and a_w. Water content (g/g-DM) is expressed as the amount of water per amount of total dry matter, including water-insoluble materials. However, a_w is mainly affected by hydrophilic materials and/or parts; there is little or no contribution from water-insoluble materials and/ or parts. Thus, the water content at each a_w value decreased intrinsically with an increase in the ratio of water-insoluble materials and/or parts. As a result, the effect of T_{gs} on the GAB parameters differed from that of the a_{wc}-predictive approach established using water-soluble carbohydrates. If the unit of equilibrium water content is changed from "g/g-DM" to "g/g-hydrophilic matters," a better a_{wc} prediction will be achieved.

CONCLUSION

In this study, we established an a_{wc}-predictive approach for amorphous water-soluble carbohydrates. This approach enabled us to predict a_{wc} from T_{gs}. In addition, the water sorption isotherm (equilibrium water content at each a_w) at 298 K could be predicted under limited conditions (below a water content of 20 g/100 g-DM). Furthermore, we demonstrated that the a_{wc}-predictive approach is also applicable to amorphous electrolytes, amorphous carbohydrate-electrolyte mixtures, and partially water-insoluble carbohydrates, depending on the ion and water-insoluble material contents. As the T_{gs} values of amorphous carbohydrates have been widely reported previously or can be readily evaluated, this predictive approach will be useful for characterizing the physical properties of amorphous carbohydrates and carbohydrate-based foods.

CONFLICTS OF INTERESTS

Appendix a

As shown in Fig. 1, the water sorption isotherm of amorphous water-soluble carbohydrates commonly exhibits type II or III curve. Type II curve can be divided into three regions. In the low a_w-region, monolayer water adsorption occurs. The monolayer water content (W_m) depends on the surface area of the carbohydrates; the higher the T_{gs}, the larger the molar mass [11,18] and thus lower the surface area per g-DM (i.e., lower W_m). In the intermediate a_w-region, multilayer water adsorption occurs, and the a_w-dependence of water content becomes too sensitive; a slight change in water content results in a large change in a_w. In the high a_w-region, the a_w-dependence of water content becomes much weaker because of the appearance of bulk water; the system behaves as an aqueous solution. Around the turning point between the low and intermediate a_w-region, glass to rubber transition is expected to occur [15]. In other words, the water content and a_w become W_c and a_{wc}, respectively, at this point. T_{gs} will be directly proportional to W_c and a_{wc}. Based on these interpretations, we expected that type II water sorption isotherm can be characterized by T_{gs}. Type III, however, is commonly observed for the amorphous water-soluble carbohydrates having a low T_{gs} (lower than or close to 298 K). Thus, we assumed that a_{wc} cannot be intrinsically defined for these materials.

REFERENCES

[1]   Sogabe T, Kawai K, Kobayashi R, Jothi JS, Hagura Y. Effects of porous structure and water plasticization on the mechanical glass transition temperature and textural properties of freeze-dried trehalose solid and cookie. J Food Eng. 2018; 217: 101−7.

[2]   Sogabe T, Kobayashi R, Thanatuksorn P, Suzuki T, Kawai K. Physical and structural characteristics of starch-based and conventional cookies: Water sorption, mechanical glass transition, and texture properties of their crust and crumb. J Texture Stud. 2021; 52: 347−57.

[3]   Fongin S, Alvino Granados AE, Harnkarnsujarit N, Hagura Y, Kawai K. Effects of maltodextrin and pulp on the water sorption, glass transition, and caking properties of freeze-dried mango powder. J Food Eng. 2019; 247: 95−103.

[4]   Fongin S, Kawai K, Harnkarnsujarit N, Hagura Y. Effects of water and maltodextrin on the glass transition temperature of freeze-dried mango pulp and an empirical model to predict plasticizing effect of water on dried fruits. J Food Eng. 2017; 210: 91−7.

[5]   Alvino Granados AE, Mochizuki T, Kawai K. Effect of glass transition temperature range on the caking behavior of freeze-dried carbohydrate blend powders. Food Eng Rev. 2021; 13: 204−14.

[6]   Alvino Granados AE, Kawai K. Browning, Starch gelatinization, water sorption, glass transition, and caking properties of freeze-dried Maca (*Lepidium meyenii* Walpers) Powders. J Appl Glycosci. 2020; 67: 111−7.

[7]   Alvino Granados AE, Kawai K. Effect of cellulose powder content on the water sorption, glass transition, mechanical relaxation, and caking of freeze-dried carbohydrate blend and food powders. LWT 2021; 148: 111798.

[8]   Alvino Granados AE, Fongin S, Hagura Y, Kawai K. Continuously distributed glass transition of maca (*Lepidium meyenii* Walpers) powder and impact on caking properties. Food Biophys. 2019; 14: 437−45.

[9]   Roos YH. Water activity and physical state effects on amorphous food stability. J Food Process Preserv. 1993; 16: 433−47.

[10] Sillick M, Gregson CM. Critical water activity of disac-

charide/maltodextrin blends. Carbohydr Polym. 2010; 79: 1028−33.

[11] Kashiwakura Y, Sogabe T, Hiyama Y, Arakawa N, Fujii T, Tochio T, et al. Prediction and control of glass transition temperature for hydrogenated starch hydrolysates and its impact on the texture modification of gummy. Food Hydrocoll. 2021; 126: 107467.

[12] Roos YH. Phase Transitions in Foods. 1st edition. San Diego: Elsevier; 1995.

[13] Johari GP, Hallbrucker A, Mayer E. The glass-liquid transition of hyperquenched water. Nature. 1987; 330: 552−3.

[14] Sastry S. Going strong or falling apart? Nature. 1999; 398: 467−70.

[15] Carter BP, Schmidt SJ. Developments in glass transition determination in foods using moisture sorption isotherms. Food Chem. 2012; 132: 693−8.

[16] Bouquerand PE, Maio S, Meyer F, Normand V. Moisture stability of maltodextrin-based delivery systems. Food Biophys. 2008; 3: 182−5.

[17] Fukami K, Kawai K, Takeuchi S, Harada Y, Hagura Y. Effect of water content on the glass transition temperature of calcium maltobionate and its application to the characterization of non-Arrhenius viscosity behavior. Food Biophys. 2016; 11: 410−6.

[18] Kawai K, Fukami K, Thanatuksorn P, Viriyarattanasak C, Kajiwara K. Effects of moisture content, molecular weight, and crystallinity on the glass transition temperature of inulin. Carbohydr Polym. 2011; 83: 934−9.

[19] Fabra MJ, Márquez E, Castro D, Chiralt A. Effect of maltodextrins in the water-content-water activity-glass transition relationships of noni (*Morinda citrifolia* L.) pulp powder. J Food Eng. 2011; 103: 47−51.

[20] Rahman MS, Al-Belushi RH. Dynamic isopiestic method (DIM): Measuring moisture sorption isotherm of freeze-dried garlic powder and other potential uses of DIM. Int J Food Prop. 2006; 9: 421−37.

[21] Samaniego-Esguerra CM, Boag IF, Robertson GL. Comparison of regression methods for fitting the GAB model to the moisture isotherms of some dried fruit and vegetables. J Food Eng. 1991; 13: 115−33.

[22] Tsami E, Krokida MK, Drouzas AE. Effect of drying method on the sorption characteristics of model fruit powders. J Food Eng. 1998; 38: 381−92.

[23] Kim SS, Kim SY, Kim DW, Shin SG, Chang KS. Moisture sorption characteristics of composite foods filled with strawberry jam. Lwt 1998; 31: 397−401.

[24] Myhara RM, Sablani SS, Al-Alawi SM, Taylor MS. Water sorption isotherms of dates: Modeling using GAB equation and artificial neural network approaches. LWT - Food Sci. Technol. 1998; 31: 699−706.

[25] Timmermann EO, Chirife J, Iglesias HA. Water sorption isotherms of foods and foodstuffs: BET or GAB parameters? J Food Eng. 2001; 48: 19−31.

[26] Foster KD, Bronlund JE, Paterson AHJ (Tony). Glass transition related cohesion of amorphous sugar powders. J Food Eng. 2006; 77: 997−1006.

[27] Kawai K, Hagiwara T, Takai R, Suzuki T. Comparative investigation by two analytical approaches of enthalpy relaxation for glassy glucose, sucrose, maltose, and trehalose. Pharm Res. 2005; 22: 490−5.

[28] Haque MK, Kawai K, Suzuki T. Glass transition and enthalpy relaxation of amorphous lactose glass. Carbohydr Res. 2006; 341: 1884−9.

[29] Fukami K, Takeuchi S, Fukujyu T, Hagura Y, Kawai K. Water sorption, glass transition, and freeze-concentrated glass-like transition properties of calcium maltobionate–maltose mixtures. J Therm Anal Calorim. 2019; 135: 2775−81.